Current Neurology and Neuroscience Reports (2019) 19: 42
https://doi.org/10.1007/s11910-019-0961-8

NEUROIMAGING (N PAVESE, SECTION EDITOR)

Neuroimaging Technological Advancements for Targeting in Functional Neurosurgery

Alexandre Boutet[1,2] · Robert Gramer[2] · Christopher J. Steele[3,4] · Gavin J. B. Elias[2] · Jürgen Germann[2] · Ricardo Maciel[2,5] · Walter Kucharczyk[1,2] · Ludvic Zrinzo[6] · Andres M. Lozano[2] · Alfonso Fasano[7,8,9]

Published online: 30 May 2019

Abstract

Purpose of Review Ablations and particularly deep brain stimulation (DBS) of a variety of CNS targets are established therapeutic tools for movement disorders. Accurate targeting of the intended structure is crucial for optimal clinical outcomes. However, most targets used in functional neurosurgery are sub-optimally visualized on routine MRI. This article reviews recent neuroimaging advancements for targeting in movement disorders.

Recent Findings Dedicated MRI sequences can often visualize to some degree anatomical structures commonly targeted during DBS surgery, including at 1.5-T field strengths. Due to recent technological advancements, MR images using ultra-high magnetic field strengths and new acquisition parameters allow for markedly improved visualization of common movement disorder targets. In addition, novel neuroimaging techniques have enabled group-level analysis of DBS patients and delineation of areas associated with clinical benefits. These areas might diverge from the conventionally targeted nuclei and may instead correspond to white matter tracts or hubs of functional networks.

Summary Neuroimaging advancements have enabled improved direct visualization-based targeting as well as optimization and adjustment of conventionally targeted structures.

Keywords Deep brain stimulation · Functional neurosurgery · MRI · Neuroimaging

Introduction

A wide range of brain disorders are thought to arise from abnormal neural activity in brain circuits. Deep brain stimulation (DBS) is a surgical treatment directed toward modulating dysfunctional circuits [1]. During DBS surgery, electrodes are inserted into precise brain structures, usually part of the underlying aberrant circuit. For example, in Parkinson's disease (PD), the most commonly targeted brain structure is the subthalamic nucleus (STN), an essential hub in the brain's motor circuitry [2]. The globus pallidus interna (GPi) is also a target in PD, however less often used [3]. The thalamic ventral intermediate (VIM) nucleus and GPi are commonly used for essential tremor and dystonia, respectively [4]. The

This article is part of the Topical Collection on *Neuroimaging*

✉ Alfonso Fasano
alfonso.fasano@uhn.ca; alfonso.fasano@gmail.com

[1] Joint Department of Medical Imaging, University of Toronto, Toronto, ON, Canada

[2] University Health Network, Toronto, ON, Canada

[3] Department of Psychology, Concordia University, Montreal, Quebec, Canada

[4] Department of Neurology, Max Planck Institute for Human Cognitive and Brain Sciences, Leipzig, Germany

[5] Division of Neurology, Edmond J. Safra Program in Parkinson's Disease, Morton and Gloria Shulman Movement Disorders Clinic, Toronto Western Hospital, UHN University of Toronto, Toronto, Ontario, Canada

[6] Functional Neurosurgery Unit, Department of Clinical and Movement Neurosciences, University College London, Queen Square Institute of Neurology, London, UK

[7] University Health Network, Toronto, ON, UK

[8] Krembil Brain Institute, Movement Disorders Centre - Toronto Western Hospital, 399 Bathurst St, 7McL410, Toronto, ON M5T 2S8, Canada

[9] Center for Advancing Neurotechnological Innovation to Application (CRANIA), Toronto, ON, Canada

same brain areas are targets for ablative treatments with radiofrequency, radiation (i.e., gamma knife radiosurgery) and ultrasound (i.e., MRI-guided focused ultrasound).

Although clinical benefits produced via DBS are best known in movement disorders such as PD, dystonia, and tremor, there is mounting evidence that DBS neuromodulation has its place in treating psychiatric and cognitive disorders [1, 4]. The therapeutic effects achieved with DBS hinge upon selective stimulation of the intended structure through accurate and precise placement of the electrodes—maximizing therapeutic benefits while minimizing spillover onto neighboring structures that may produce adverse effects [5, 6]. Despite significant advances in neuroimaging technology over the past decades, routinely acquired preoperative brain magnetic resonance imaging (MRI) sequences remain deficient at directly visualizing DBS targets for stereotactic planning purposes [7, 8]. Some groups have developed dedicated MRI sequences that visualize some of the anatomical structures commonly targeted during DBS surgery on MRI at 1.5-T field strengths such as the STN [9–12] and the posteroventral GPi [13, 14]. Nevertheless, some commonly used targets, such as the VIM, cannot be visualized on 1.5-T structural MRI, and many groups have continued to use indirect targeting methods when performing DBS—relying on identifiable surrogate anatomical landmarks and coupled with other techniques such as intraoperative microelectrode recordings (MER) and/or clinical evaluation in awake patients [15].

While neuroimaging plays a central role in today's DBS surgery, it was not until the 1940s that it was used to guide stereotaxic surgeries targeting a precise brain structure via a coordinate system. Spiegel et al. (1947) [16] and Tasker (1965) [17] pioneered stereoencephalography to triangulate brain structures through radiographic skull landmarks. As computerized tomography (CT) and MRI became widely available, their ability to non-invasively discern internal brain structures made them gold standards for DBS preoperative planning. Drawing from atlases with a defined coordinate system, relationships between targets and anatomical landmarks such as the anterior and posterior commissures are still used to plan DBS surgeries [15]. The known inter-surgeon variability when identifying these landmarks is problematic, however [18]. Current neurosurgical technique entails combining indirect, coordinate-based targeting and MRI-guided direct target visualization. In many cases, this standard planning is further supplemented with intraoperative techniques such as MERs and clinical stimulation to produce motor, sensory, physiologic, or cognitive phenomena [15, 19, 20].

In this review, we will summarize the recent neuroimaging technological advancements and their utility as new methods for optimizing targeting in functional neurosurgery. First, technological developments including ultra-high-field (UHF) MRI and novel MRI pulse sequences and image processing methods allowing improved target visualization will be discussed. Then, refinement of current DBS targets for movement disorders based on structural and functional connectomes will be reviewed.

Direct Target Visualization with Ultra-high-field MR Imaging

While acquisition of 3 Tesla (3 T) MRI for clinical neuroimaging has become routine in most neurological and neurosurgical centers, thanks to technological advances, UHF (i.e., 7 T) MRI are becoming increasingly available [21, 22]. Compared to the widely used 1.5 T MRI in the 1990s, when planning DBS surgery for movement disorders, 3-T MRI offers superior visualization of the targets [23–25]. Lower field strength MRI may be used for intra-operative validation of targeting accuracy [10•, 26, 27]. The net benefit of using UHF MRI in comparison to 3 T is still being investigated.

From a physics standpoint, a higher magnetic field strength offers clear advantages while also introducing disadvantages that must be acknowledged (Table 1). The main benefit of using UHF is the desirable increase in signal-to-noise ratio (SNR) [22, 28–30], which theoretically grows linearly in relation to magnetic field strength [23, 24]. Higher SNR in turn allows increased spatial resolution, permitting the visualization and delineation of smaller neuroanatomical structures (Table 1). Such precision is warranted as structures of interest targeted with DBS in movement disorders are generally sub-centimeter in scale [31]. Naturally, as the spatial resolution inherent to lower magnetic field strength approaches or is inferior to the dimensions of the desired structure, MRI volume averaging leads to blurring of the anatomy. Also, optimal SNR is particularly relevant in DBS planning since it scales inversely with distance from the cortex [29, 32]. Moreover, due to the non-uniform distribution of SNR throughout the head at UHF MRI, SNR of deep structures has been shown to particularly improve with increasing magnetic field strengths [33]. Importantly, there is little trade-off in terms of acquisition times at UHF MRI; incorporating similar protocols to those used in current clinical imaging, UHF MRI can acquire smoother, less grainy images than those obtained at lower field strengths in a comparable timeframe [8, 21, 23]. For example, diagnostic quality T1-weigthed (T1W) and T2-weighted (T2W) 7-T images can both be obtained within 10 min [8]. In addition to improved SNR, UHF MRI is reported to confer a better contrast-to-noise ratio (CNR), improving the ability to differentiate two small abutting structures [22, 29]. Given that the STN is bordered by several small structures such as the ansa lenticularis, zona incerta, and substantia nigra, this capacity becomes crucial [34]. Additionally, while increased susceptibility artifacts may be a problem with UHF MRI (as discussed in the next paragraphs), it may also be an advantage to better visualize iron-rich structures such as the STN [8, 35•, 36]. By reducing the gap between MRI and

Table 1 Advantages, disadvantages, and future developments of the reviewed neuroimaging advancements

	Advantages	Disadvantages	Future developments
UHF MRI	1. Higher SNR	1. Lack of availability	1. Higher magnetic field strengths (e.g., 9 T)
	2. Higher spatial resolution	2. Image distortion	2. Correction of image distortion
	3. Increased susceptibility artifacts (e.g., better for iron-rich structures)	3. Increased susceptibility artifacts (e.g., distortions)	3. Development of coils and equipment that allow acquisition of stereotactic images
		4. Requirement for image co-registration with another stereotactic imaging modality	
		5. Safety concerns with metallic implants	
		6. Specialized knowledgebase and clinical expertise	
New MRI pulse sequences (e.g., QSM)	1. Better contrast between small structures	1. Imaging preprocessing	1. Integration into commercial software
	2. No need for purchase of expensive new equipment	2. Specialized knowledgebase and clinical expertise	2. Development of coils and equipment that allow acquisition of stereotactic images
	3. More easily incorporated into existing surgical workflows	3. Not always possible to perform with commercially available stereotactic frames	
Targeting connectomes	1. Refine current targets	1. Functional neuroimaging acquisition	1. Prospective validation
	2. Direct visualization of target (e.g., tracts)	2. Specialized knowledgebase and clinical expertise	2. Improved MRI pulse sequences
		3. Requirement for image co-registration with another stereotactic imaging modality	
Probabilistic maps for targeting	1. Refined current targets	1. Large patient cohorts required	1. Prospective validation
	2. Data-driven approach	2. Specialized knowledgebase and clinical expertise	2. Refined VTA modeling
	3. Direct visualization of target (e.g., maps)	3. Requirement for image co-registration with another stereotactic imaging modality	

UHF MRI, ultra-high-field MRI; *MRI*, magnetic resonance imaging; *SNR*, signal-to-noise ratio; *QSM*, quantitative susceptibility imaging

histology, this increased spatial resolution opens the door to highly accurate and detailed MRI atlases [31, 37, 38], thus further refining the surgeon's ability to target a specific territory within a given circuit (e.g., the dorso-lateral STN involved in motor functions).

Recent studies have investigated the validity of UHF MRI in the context of DBS surgery for movement disorders. UHF allows visualization of otherwise obscure (or indiscernible) brain structures on clinical 1.5-T or 3-T MRI [22, 28, 34, 39, 40, 41•, 42•, 43]. At these commonly used field strengths, 3 T has been reported to provide STN visualization (to some degree) for PD DBS [24], which has been shown to correlate well with MER recordings [25••]. With its far superior SNR and spatial resolution, UHF-imaging permits accurate delineation of STN borders. Indeed, UHF-demarcated STN borders have already been shown to correlate well with MER recordings [28], although a slight discrepancy between the two sources of information was described in another study [43], highlighting the possible image distortions at UHF MRI. However, these small discrepancies could also be explained by distortion of brain tissue by the advancing surgical probes. On the other hand, the fact that clinical outcomes have been shown to correlate with the proportion of stimulation overlapping the STN at 7 T partly validates the accurate anatomical representation of UHF MRI [28]. At higher magnetic field strengths, STN can also be segmented and parcellated based upon white matter projections, raising the prospect of precise, substructure level targeting of previously indiscernible areas (i.e., the motor division of STN) [41•]. This direct visualization of DBS targets may improve surgical techniques and clinical outcome given inter-individual variability in STN location has been reported [28].

UHF MRI may also hold promise for essential tremor DBS, which most commonly targets the motor thalamus [1]. Indeed, the potential benefits here may even be more pronounced than those for PD; while the STN may be adequately visualized on routinely acquired MRI [7], the thalamic intranuclei, including the VIM, are not appreciated at all on current MRI protocols. These nuclei can be visualized with appropriate MRI sequences at 7-T MRI [40, 42•], however, which is a notable advantage when planning DBS surgery for tremor.

Although UHF MRI can theoretically provide substantial advantages, there are only about 60 centers worldwide at present; as such, the poor availability of this technology remains a barrier to mainstream clinical practice (Table 1) [22]. Additionally, higher magnetic field strengths are more prone to susceptibility artifacts and image distortions [23, 39], leading in theory to a greater risk of mistargeting. While this limitation

would be particularly problematic for DBS surgery given the small scale of structures involved, most of the subcortical structures targeted in movement disorders are located deep in the brain and have been shown to have little distortion when compared to the routine 1.5-T MRI [44•]. Due to their proximity to the paranasal sinuses, areas such as the inferior frontal and temporal lobes are most at risk of distortion; given these are not targets for movement disorder DBS at present, the problem of UHF MRI-related distortion is of less concern here than it might be for psychiatric indications. Moreover, UHF MRI has not been reported in conjunction with a commercially available stereotactic frame; UHF MR images must therefore be co-registered with stereotactic images using another modality, a step that can introduce registration errors [45]. Lastly, from a practical standpoint, the risk of metallic implants in UHF MRI has not been thoroughly evaluated and may thus limit the clinical generalizability of this technology [30, 46, 47]. Patients with metallic implants such as aneurysm clips and cardiac metallic devices are increasingly prevalent, and safety studies, such as those recently performed with 3-T MRI and DBS [48, 49], will be needed before they can safely undergo UHF MRI.

In conclusion, UHF MRI still remains an experimental technique requiring a more specialized knowledge base and clinical expertise than is typical in the field of clinical radiology. As even higher field strengths [34] and image distortion correction methods are being developed [50–52], continued testing is required to bring the potential benefits, obstacles, and trade-offs presented by UHF MRI relative to lower field strength MRI more clearly into focus.

Direct Target Visualization with New MRI Pulse Sequences

In addition to increasing the magnetic field strength, changing MRI acquisition parameters is also a promising technique. MRI pulse sequences are designed to provide varying kinds of contrasts through their sensitivity to different tissue properties. For example, routinely acquired structural MRI pulse sequences such as T1W and T2W sequences are mostly sensitive to the time taken for the water molecules (i.e., protons) to realign with the MRI magnetic field and the time for the excited water molecules (i.e., protons) to go out of phase with each other, respectively. These sequences can usually differentiate between gray matter, white matter, and other basic components such as fat and cerebrospinal fluid. However, at lower field strengths (1.5 T or 3 T), they generally fail to delineate smaller nuclei and subnuclei. On routinely used T2W sequence, for instance, the STN appears hypointense and may be difficult to differentiate from surrounding structures [7], necessitating the use of adjunct indirect targeting methods.

In recent years, developments in MRI pulse sequences and advances in imaging processing have led to the development of sequences sensitive to other aspects of tissue composition. The STN is an iron-rich structure, which is likely responsible for its relative hypointensity on T2W imaging [36, 53]. SWI, a type of gradient echo (GRE) sequences, is highly sensitive to iron content by taking advantage of the T2* artifact associated with its paramagnetic properties [54]. These sequences can be acquired on most MRI scanners and may be incorporated into existing surgical workflows (Table 1). Not surprisingly, the STN exhibits striking hypointensity when imaged with SWI pulse sequences [25••, 36, 53]. However, the iron present in nearby structures also influences the signal in the STN, degrading the contrast and limiting the ability to differentiate the STN from its surroundings [54]. Fortunately, a novel image processing technique that can be applied to multi-echo GRE acquisitions—quantitative susceptibility mapping (QSM)—quantifies the susceptibility in each structure and represents them on a scale that enhances the contrast between neighboring structures (Table 1) [36, 53, 54]. The STN [35•, 36, 53], and (to a lesser degree) the GPi [55], have been shown to be better appreciated with QSM. With this marked increase in contrast between structures, delineation of subcortical structures such as the thalamus, GPi, and STN can be performed using an automated computer algorithm [56, 57]. Furthermore, by providing a quantifiable tissue composition signal that mainly reflects iron quantity, QSM can provide data on the expected age-related changes in small subcortical nuclei such as STN [58, 59]. Of note, QSM reconstruction requires niche expertise for the necessary image preprocessing (Table 1) [60]. Also, not all commercially available stereotactic frames may allow acquisition of GRE sequences. This pulse sequence-dependent enhancement of target area visualization may help improve current targeting approaches and decrease the number of surgical passes, enhancing practice and improving outcomes. As such, it is extremely promising and may be particularly powerful when combined with UHF MRI.

Finally, proton density–weighted MR images reflect the actual density of protons in tissues and is another sequence of interest since it provides excellent contrast between white and gray matter structures, making it useful in defining the GPi within the components of the lentiform nucleus [13] as well as the pedunculopontine nucleus [61].

Targeting Circuits of Interest

Recent research suggests that optimal structures to be targeted may not be apparent with routine structural imaging. For example, it has been suggested that the clinical benefits of DBS may be better understood as emerging from white matter pathways [62–67] or focal hubs of functional networks [68••] rather than from discrete structures such as deep gray matter nuclei. Interestingly, when these functional and structural networks are targeted more directly, the resultant target may spatially diverge from conventional coordinates, possibly reflecting various underlying neural substrates responsible for clinical benefits.

Conventionally, DBS for movement disorders has targeted discrete gray matter nuclei. Although these targets are known to be associated with clinical benefits, recent evidence suggest that entities such as white matter tracts [63, 69, 70] or functional networks [68••] may also be responsible for the therapeutic effects of DBS (Table 1). White matter tracts and functional networks cannot be visualized on routinely acquired structural MRI and require different MRI acquisition parameters to be appreciated: diffusion-weighted imaging (DWI) for tractography and resting-state functional magnetic resonance imaging (rsfMRI) for functional networks (Table 1). In some cases, newly visualized white matter pathways may be employed as independent targets for neurosurgical intervention. One example of this approach pertains to the dentato-rubro-thalamic tract, part of the cerebello-thalamo-cortical tremor network, which is being investigated as a direct DBS target for tremor using tractography methods [63, 69, 70]. A similar tactic has been adopted in the realm of neuropsychiatric DBS, with tractography-dependent targeting of the medial forebrain bundle pathway for treatment of depression [71]. Another variation is the use of white matter tracts to refine and delineate a more conventional target. This includes triangulating VIM based on the relative positions of pyramidal and medial lemniscus tracts for tremor surgery [72], and also the tract-based parcellation of the STN and thalamic nuclei into sub-regions with preferential motor connections [41•, 73]. Thus far, few DBS studies for movement disorders [63, 70] have explored the prospective application of these new techniques, although prospective targeting of white matter tracts is increasingly described in the context of other neurosurgical techniques for movement disorders [74] as well as DBS for psychiatric disorders [75, 76]. Given the substantial inter-patient variability in white matter pathways, this type of targeting is likely to be more sensitive to individual neuroanatomical differences, leading to more personalized DBS delivery [77]. However, it will be critical for investigators to remain cognizant of the bewildering variety of tractography methods, the need for rigorous methods, and the importance of visual inspection in order to stave off spurious results [78]. Also, these white matter tracts must be co-registered with stereotactic images, a step that can introduce registration errors (Table 1). Constantly evolving MRI hardware and pulse sequence designs should limit spurious results and allow visualization of structures, as of now, only seen on histology.

Data-Driven Connectome Targeting

The conventional DBS targets for movement disorders have been most commonly empirically derived from lesioning studies [79]. Although these targets provide clinical benefits in movement disorders, it is plausible that they may not be optimal. Indeed, pinpointing the effective component across the volume of lesions may have been difficult partly due to the lack of group-level analysis methods. Recent neuroimaging advances allowing (1) precise transformation of patients' brain into an average brain (i.e., non-linear normalization to Montreal Neurological Institute—MNI—brain template) [80], (2) DBS electrode localization [81••], and (3) estimation of the volume of tissue activated (VTA) [81••, 82, 83] have enabled this group-level analyses to be conducted for DBS (Fig. 1). This approach, in which probabilistic maps based on clinical outcomes are computed from regions of interest have also been performed with ablative therapies [84, 85]. Easy-to-use analysis pipelines performing electrode localization and VTA estimation are now available in commercially available (e.g., Medtronic SureTune, Medtronic Inc.; Elements, Brainlab Inc.) and research software (e.g., Lead-DBS). Once normalized in an average brain, electrode locations and VTAs from patients can be weighted with clinical outcomes to derive a cohort probabilistic maps of efficacy [86–91]. This agnostic approach is driven by clinical data provided by DBS programming, an empirical clinical process that is usually blinded to precise electrode location (Table 1). Challenging the routinely targeted structures, less conventional targets such as the posterior subthalamic areas in DBS for tremor might be suggested with such methods [87••]. Moreover, areas associated with specific clinical benefits such as tremor, rigidity, or bradykinesia in PD may now be defined, opening the door to individualized DBS targeting based on dominant disease phenotypes [86, 89]. A similar approach has also been used to delineate areas responsible for DBS adverse effects such as paresthesia and diplopia [86–88].

Computation of these maps of clinical benefits and adverse effects become highly important with the increasing use of directional leads, introducing more programming possibilities and complexity [92]. Directional lead stimulation can be preferentially directed toward the optimal target, minimizing stimulation of unwanted areas. Neuroimaging techniques using CT scan or x-rays have been developed to determine the lead orientation [93–96] and the most recent VTA modeling software can compute this steered stimulation [81••, 97] (Fig. 2). Following electrode localization and VTA modeling, clinicians can then use these tools to inform programming. Given time constraints and patient fatigue, it is impracticable to thoroughly assess a large number of stimulation parameters via clinical means; this restriction could be mitigated by using probabilistic maps of clinical outcomes and integrating them with individual patient anatomy, providing patient-specific targeting and guiding subsequent programming.

Limits of the current methods include (1) suboptimal patients' brain normalization—and thus electrode localization—of *abnormal* (e.g., markedly atrophic) brains; (2) limited VTA modeling, which does not take stimulation frequency or pulse width into account and typically makes assumptions about electrode-tissue impedance; and (3) the large number of patients required for robust results (Table 1).

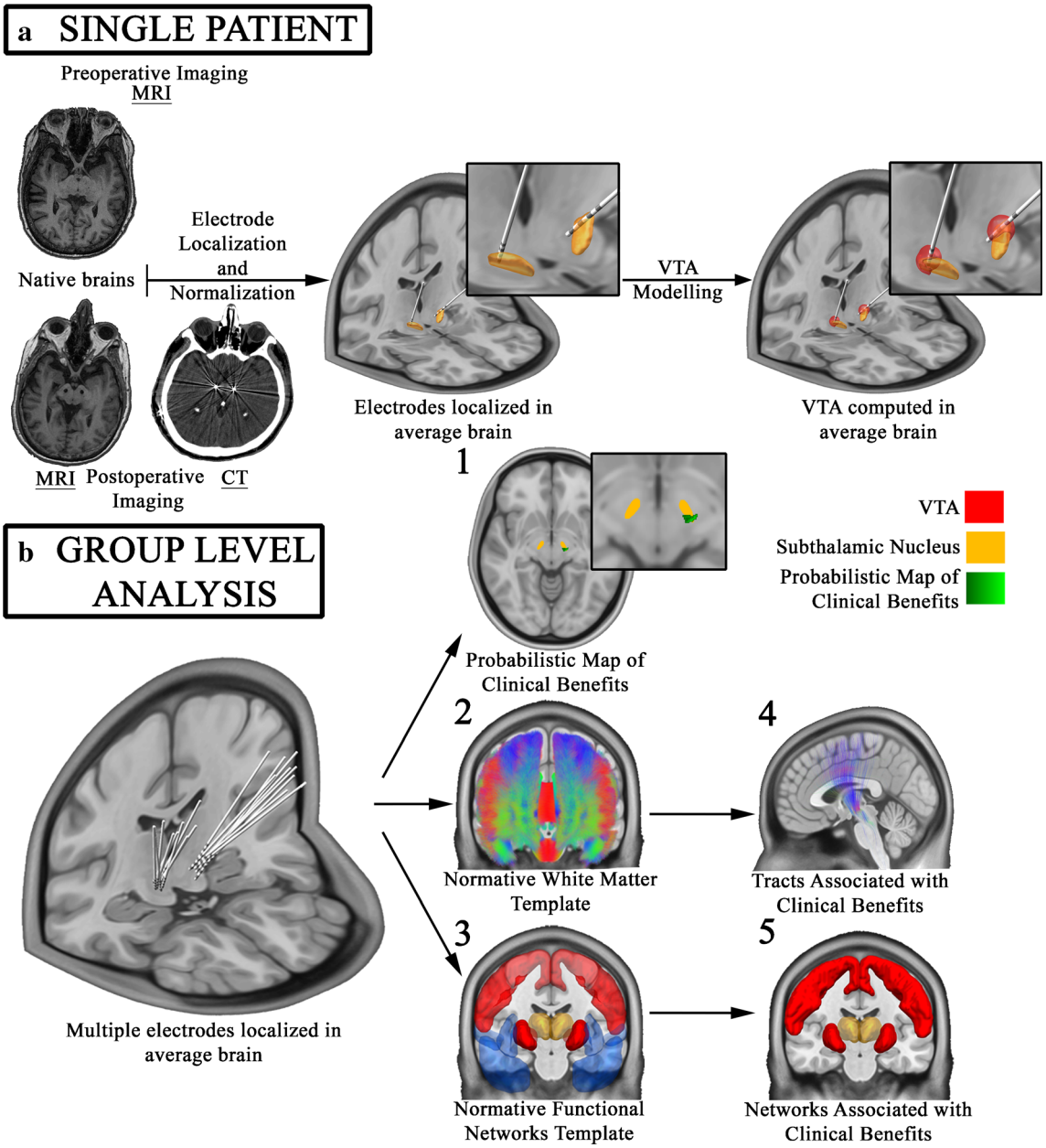

Fig. 1 Neuroimaging pipeline methods for single (**a**) and group (**b**) level analysis in DBS patients. **a** Using preoperative and postoperative MRI (or postoperative CT) native brain scans, DBS electrodes are localized and transformed into an average brain (e.g., MNI brain). Using the computed VTA, the stimulated structures in a single patient can then be investigated. **b** Following normalization and electrode localization of a cohort of DBS patients, each patient VTA can be weighted by clinical scores and a probabilistic map of clinical benefits can be computed on a structural MRI (1: axial T1W MNI brain MRI). Using the weighted VTA, publicly available normative dataset of white matter tracts (2) and functional networks (3) can be used to investigate connections associated with clinical benefits (or adverse effects) (4, 5). MRI, magnetic resonance imaging; CT, computerized tomography; MNI, Montreal Neurological Institute; STN, subthalamic nucleus; VTA, volume of tissue activated; T1W, T1-weighted

In addition to defining probabilistic areas of clinical benefits and adverse effects, probabilistic group-level approaches can also leverage normative connectomes to explore the network connectivity associated with desired and undesired outcomes. Since the vast majority of DBS patients do not undergo DWI and rsfMRI imaging, probabilistic areas of clinical benefits could—until recently—only be described and computed using routinely acquired structural scans. Now, however, neuroimaging techniques have permitted the aggregation of large DWI and rsfMRI datasets derived from healthy subjects into publicly available, standard space such as the MNI brain template. While native patient imaging may better reflect the underlying patient-specific connectivity, state-of-the-art normative data gathered through initiatives such as the Human Connectome Project and Brain Genomics Superstruct Project offer unparalleled spatial resolution and

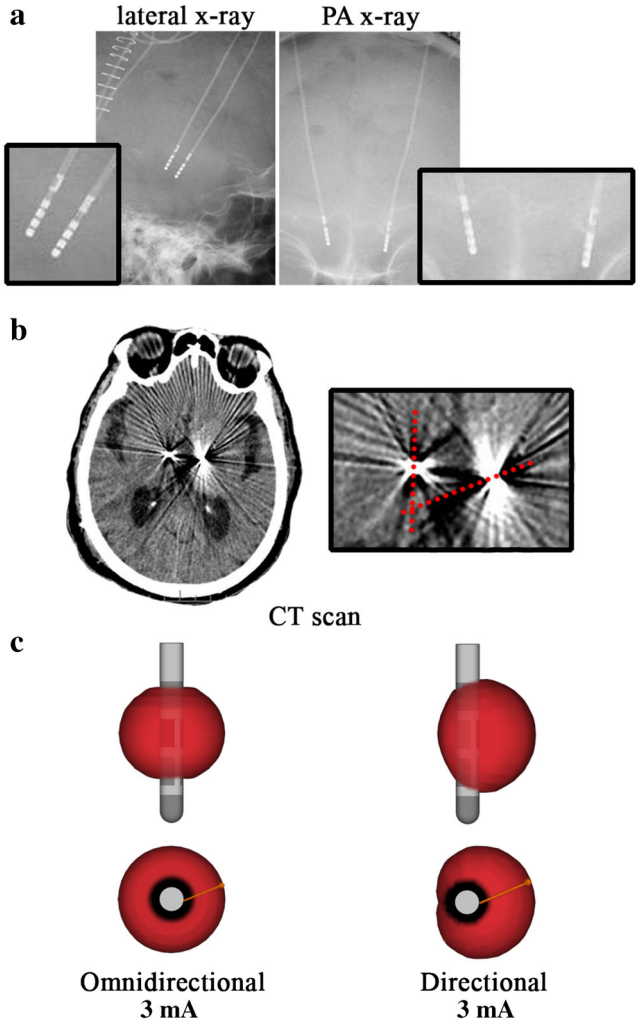

Fig. 2 Directional lead localization and VTA computation. **a** General orientation of the directional lead is estimated with the radiopaque marker on skull x-rays. **b** Precise orientation of the directional lead is computed with the CT artifact (dotted red lines). **c** Computation of omnidirectional VTA (left) and directional VTA (right) based on the orientation of the directional lead (STIMVIEW, Boston Scientific). The orange line shows the orientation of the radiopaque marker. VTA, volume of tissue activated mA, milliampere

signal-to-noise ratio [68••, 98, 99]. Once electrode localizations and VTA modeling have been performed and the resulting constructs have been normalized to an average brain (e.g., MNI brain), each VTA can be employed as a seed in the normative templates to investigate associated white matter pathways and functional networks (Fig. 1). In other words, by tapping into high-quality, publicly available, normative datasets, it is now possible to explore white matter pathways and functional networks associated with best clinical outcomes using only routinely acquired neuroimaging data. It is not yet clear whether native patient DWI and rsfMRI sequences will reveal individual variability that leads to meaningful clinical benefit. Nevertheless, although the normative dataset approach is only a recent development, it is already providing encouraging results and as recently been described by A. Horn [100]. Normative connectomic mapping has been shown to predict clinical outcomes in both PD DBS patients with STN electrodes [68••] and in psychiatric DBS patients [101], for instance. Ultimately, the probabilistic zones and networks identified by these analyses in an average brain could then be transformed to the native patients' brain in order to guide preoperative planning in a manner that is both personalized and driven by large retrospective clinical outcome datasets.

Conclusions

Although neuroimaging techniques used for preoperative DBS planning have evolved—from stereoencephalogram to MRI—over the years, indirect anatomical landmarks remain indispensable to some conventional targeting paradigms. Historical and empirical DBS targets have yet to be refined. The expansive and growing cohort of movement disorder patients treated with DBS coupled with newly available neuroimaging techniques offer the opportunity to perform group analyses and better resolve which structures impart the greatest clinical benefits (or adverse effects) to patients. While traditionally targeted gray matter nuclei might play a role in the therapeutic effects of DBS, there is mounting evidence that white matter pathways and functional networks, entities typically occult on routinely acquired structural imaging, are notably involved in disease pathophysiology, and thus must be more earnestly considered in targeting. Using this new data, it is possible to consider personalized medicine in the context of DBS surgery for movement disorders. Given the newly available neuroimaging technologies, individualized targeting methods should be used. Furthermore, depending on the disease phenotype, it is also sensible that slight variations of the same target may confer more optimal benefits. These new technologies should allow progress toward patient individualized targeting, better definition of established surgical targets, and, possibly, discovery of new ones.

Compliance with Ethical Standards

Conflict of Interest Alexandre Boutet, Robert Gramer, Christopher J. Steele, Gavin J. B. Elias, Jürgen Germann, Ricardo Maciel, Walter Kucharczyk each declare no potential conflicts of interest. Ludvic Zrinzo reports honoraria for presenting educational material at meetings from Medtronic and Boston Scientific, outside the submitted work. Andres M. Lozano reports personal fees from Medtronic, St Jude, and Boston Scientific and Functional Neuromodulation, during the conduct of the study, and grants from GE Healthcare, outside the submitted work. Alfonso Fasano reports grants, personal fees, and non-financial support from Abbvie; grants, personal fees, and non-financial support from Medtronic; grants and personal fees from Boston Scientific; personal fees from Sunovion; personal fees from Chiesi farmaceutici; personal fees from UCB; and grants and personal fees from Ipsen, outside the submitted work.

Human and Animal Rights and Informed Consent This article does not contain any studies with human or animal subjects performed by any of the authors.

References

Papers of particular interest, published recently, have been highlighted as:
- • Of importance
- •• Of major importance

1. Lozano AM, Lipsman N. Probing and regulating dysfunctional circuits using deep brain stimulation. Neuron. 2013;77(3):406–24. https://doi.org/10.1016/j.neuron.2013.01.020.
2. Okun MS. Deep-brain stimulation for Parkinson's disease. N Engl J Med. 2012;367(16):1529–38. https://doi.org/10.1056/NEJMct1208070.
3. Follett KA, Weaver FM, Stern M, Hur K, Harris CL, Luo P, et al. Pallidal versus subthalamic deep-brain stimulation for Parkinson's disease. N Engl J Med. 2010;362(22):2077–91. https://doi.org/10.1056/NEJMoa0907083.
4. Lozano AM, Lipsman N, Bergman H, Brown P, Chabardes S, Chang JW, et al. Deep brain stimulation: current challenges and future directions. Nat Rev Neurol. 2019;15:148–60. https://doi.org/10.1038/s41582-018-0128-2.
5. Li Z, Zhang JG, Ye Y, Li X. Review on factors affecting targeting accuracy of deep brain stimulation electrode implantation between 2001 and 2015. Stereotact Funct Neurosurg. 2016;94(6):351–62. https://doi.org/10.1159/000449206.
6. Bot M, Schuurman PR, Odekerken VJJ, Verhagen R, Contarino FM, De Bie RMA, et al. Deep brain stimulation for Parkinson's disease: defining the optimal location within the subthalamic nucleus. J Neurol Neurosurg Psychiatry. 2018;89(5):493–8. https://doi.org/10.1136/jnnp-2017-316907.
7. Ranjan M, Boutet A, Xu DS, Lozano CS, Kumar R, Fasano A, et al. Subthalamic nucleus visualization on routine clinical preoperative MRI scans: a retrospective study of clinical and image characteristics predicting its visualization. Stereotact Funct Neurosurg. 2018;96(2):120–6. https://doi.org/10.1159/000488397.
8. Abosch A, Yacoub E, Ugurbil K, Harel N. An assessment of current brain targets for deep brain stimulation surgery with susceptibility-weighted imaging at 7 tesla. Neurosurgery. 2010;67(6):1745–1756; discussion 56. 10.1227/NEU.0b013e3181f74105.
9. Bejjani BP, Dormont D, Pidoux B, Yelnik J, Damier P, Arnulf I, et al. Bilateral subthalamic stimulation for Parkinson's disease by using three-dimensional stereotactic magnetic resonance imaging and electrophysiological guidance. J Neurosurg. 2000;92(4):615–25. https://doi.org/10.3171/jns.2000.92.4.0615.
10. • Foltynie T, Zrinzo L, Martinez-Torres I, Tripoliti E, Petersen E, Holl E, et al. MRI-guided STN DBS in Parkinson's disease without microelectrode recording: efficacy and safety. J Neurol Neurosurg Psychiatry. 2011;82(4):358–63. https://doi.org/10.1136/jnnp.2010.205542 **These authors report MRI-guided STN DBS in Parkinson's disease patients (without MERs) with good clinical benefits and very low morbidity**.
11. Hariz MI, Krack P, Melvill R, Jorgensen JV, Hamel W, Hirabayashi H, et al. A quick and universal method for stereotactic visualization of the subthalamic nucleus before and after implantation of deep brain stimulation electrodes. Stereotact Funct Neurosurg. 2003;80(1–4):96–101. https://doi.org/10.1159/000075167.
12. Patel NK, Plaha P, Gill SS. Magnetic resonance imaging-directed method for functional neurosurgery using implantable guide tubes. Neurosurgery. 2007;61(5 Suppl 2):358–365; discussion 65-6. https://doi.org/10.1227/01.neu.0000303994.89773.01.
13. Hirabayashi H, Tengvar M, Hariz MI. Stereotactic imaging of the pallidal target. Mov Disord. 2002;17(Suppl 3):S130–4.
14. Reich CA, Hudgins PA, Sheppard SK, Starr PA, Bakay RA. A high-resolution fast spin-echo inversion-recovery sequence for preoperative localization of the internal globus pallidus. AJNR Am J Neuroradiol. 2000;21(5):928–31.
15. Lozano CS, Ranjan M, Boutet A, Xu DS, Kucharczyk W, Fasano A, et al. Imaging alone versus microelectrode recording-guided targeting of the STN in patients with Parkinson's disease. J Neurosurg. 2018;2018:1–6. https://doi.org/10.3171/2018.2.JNS172186.
16. Spiegel EA, Wycis HT, Marks M, Lee AJ. Stereotaxic apparatus for operations on the human brain. Science. 1947;106(2754):349–50. https://doi.org/10.1126/science.106.2754.349.
17. Tasker RR. Simple localization for stereoencephalotomy using the "portable" central beam of the image intensifier. Confin Neurol. 1965;26(3):209–12.
18. Pallavaram S, Yu H, Spooner J, D'Haese PF, Bodenheimer B, Konrad PE, et al. Intersurgeon variability in the selection of anterior and posterior commissures and its potential effects on target localization. Stereotact Funct Neurosurg. 2008;86(2):113–9. https://doi.org/10.1159/000116215.
19. Aviles-Olmos I, Kefalopoulou Z, Tripoliti E, Candelario J, Akram H, Martinez-Torres I, et al. Long-term outcome of subthalamic nucleus deep brain stimulation for Parkinson's disease using an MRI-guided and MRI-verified approach. J Neurol Neurosurg Psychiatry. 2014;85(12):1419–25. https://doi.org/10.1136/jnnp-2013-306907.
20. Zrinzo L, Hariz M, Hyam JA, Foltynie T, Limousin P. Letter to the editor: a paradigm shift toward MRI-guided and MRI-verified DBS surgery. J Neurosurg. 2016;124(4):1135–7. https://doi.org/10.3171/2015.9.JNS152061.
21. Forstmann BU, Isaacs BR, Temel Y. Ultra high field MRI-guided deep brain stimulation. Trends Biotechnol. 2017;35(10):904–7. https://doi.org/10.1016/j.tibtech.2017.06.010.
22. Springer E, Dymerska B, Cardoso PL, Robinson SD, Weisstanner C, Wiest R, et al. Comparison of routine brain imaging at 3 T and 7 T. Investig Radiol. 2016;51(8):469–82. https://doi.org/10.1097/RLI.0000000000000256.
23. Chandran AS, Bynevelt M, Lind CR. Magnetic resonance imaging of the subthalamic nucleus for deep brain stimulation. J Neurosurg. 2016;124(1):96–105. https://doi.org/10.3171/2015.1.JNS142066.
24. Cheng CH, Huang HM, Lin HL, Chiou SM. 1.5T versus 3T MRI for targeting subthalamic nucleus for deep brain stimulation. Br J Neurosurg. 2014;28(4):467–70. https://doi.org/10.3109/02688697.2013.854312.
25. •• Lefranc M, Derrey S, Merle P, Tir M, Constans JM, Montpellier D, et al. High-resolution 3-dimensional T2*-weighted angiography (HR 3-D SWAN): an optimized 3-T magnetic resonance imaging sequence for targeting the subthalamic nucleus. Neurosurgery. 2014;74(6):615–26. https://doi.org/10.1227/NEU.0000000000000319 **This study demonstrates improved STN visualization with 3-T MRI and optimized acquisition parameters.**
26. Warnke P. Deep brain stimulation: awake or asleep: it comes with a price either way. J Neurol Neurosurg Psychiatry. 2018;89(7):672. https://doi.org/10.1136/jnnp-2017-315710.
27. Ostrem JL, Ziman N, Galifianakis NB, Starr PA, Luciano MS, Katz M, et al. Clinical outcomes using ClearPoint interventional

MRI for deep brain stimulation lead placement in Parkinson's disease. J Neurosurg. 2016;124(4):908–16. https://doi.org/10.3171/2015.4.JNS15173.

28. Duchin Y, Shamir RR, Patriat R, Kim J, Vitek JL, Sapiro G et al. Patient-specific anatomical model for deep brain stimulation based on 7 tesla MRI. PLoS One 2018;13(8):e0201469. 10.1371/journal.pone.0201469.
29. Forstmann BU, de Hollander G, van Maanen L, Alkemade A, Keuken MC. Towards a mechanistic understanding of the human subcortex. Nat Rev Neurosci. 2016;18(1):57–65. https://doi.org/10.1038/nrn.2016.163.
30. Kraff O, Quick HH. 7T: physics, safety, and potential clinical applications. J Magn Reson Imaging. 2017;46(6):1573–89. https://doi.org/10.1002/jmri.25723.
31. Ewert S, Plettig P, Li N, Chakravarty MM, Collins DL, Herrington TM, et al. Toward defining deep brain stimulation targets in MNI space: a subcortical atlas based on multimodal MRI, histology and structural connectivity. Neuroimage. 2018;170:271–82. https://doi.org/10.1016/j.neuroimage.2017.05.015.
32. Wiggins GC, Polimeni JR, Potthast A, Schmitt M, Alagappan V, Wald LL. 96-channel receive-only head coil for 3 Tesla: design optimization and evaluation. Magn Reson Med. 2009;62(3):754–62. https://doi.org/10.1002/mrm.22028.
33. Ugurbil K. Magnetic resonance imaging at ultrahigh fields. IEEE Trans Biomed Eng. 2014;61(5):1364–79. https://doi.org/10.1109/TBME.2014.2313619.
34. Massey LA, Miranda MA, Zrinzo L, Al-Helli O, Parkes HG, Thornton JS, et al. High resolution MR anatomy of the subthalamic nucleus: imaging at 9.4 T with histological validation. Neuroimage. 2012;59(3):2035–44. https://doi.org/10.1016/j.neuroimage.2011.10.016.
35.• Alkemade A, de Hollander G, Keuken MC, Schafer A, Ott DVM, Schwarz J, et al. Comparison of T2*-weighted and QSM contrasts in Parkinson's disease to visualize the STN with MRI. PLoS One. 2017;12(4):e0176130. https://doi.org/10.1371/journal.pone.0176130 **This study shows that QSM is optimal to visualize the STN compared to the more commonly used T2W*-weighted sequences**.
36. Liu T, Eskreis-Winkler S, Schweitzer AD, Chen W, Kaplitt MG, Tsiouris AJ, et al. Improved subthalamic nucleus depiction with quantitative susceptibility mapping. Radiology. 2013;269(1):216–23. https://doi.org/10.1148/radiol.13121991.
37. Tullo S, Devenyi GA, Patel R, Park MTM, Collins DL, Chakravarty MM. Warping an atlas derived from serial histology to 5 high-resolution MRIs. Sci Data. 2018;5:180107. https://doi.org/10.1038/sdata.2018.107.
38. Keuken MC, Bazin PL, Crown L, Hootsmans J, Laufer A, Muller-Axt C, et al. Quantifying inter-individual anatomical variability in the subcortex using 7 T structural MRI. Neuroimage. 2014;94:40–6. https://doi.org/10.1016/j.neuroimage.2014.03.032.
39. Dammann P, Kraff O, Wrede KH, Ozkan N, Orzada S, Mueller OM, et al. Evaluation of hardware-related geometrical distortion in structural MRI at 7 Tesla for image-guided applications in neurosurgery. Acad Radiol. 2011;18(7):910–6. https://doi.org/10.1016/j.acra.2011.02.011.
40. Kanowski M, Voges J, Buentjen L, Stadler J, Heinze HJ, Tempelmann C. Direct visualization of anatomic subfields within the superior aspect of the human lateral thalamus by MRI at 7T. AJNR Am J Neuroradiol. 2014;35(9):1721–7. https://doi.org/10.3174/ajnr.A3951.
41.• Plantinga BR, Temel Y, Duchin Y, Uludag K, Patriat R, Roebroeck A, et al. Individualized parcellation of the subthalamic nucleus in patients with Parkinson's disease with 7T MRI. Neuroimage. 2018;168:403–11. https://doi.org/10.1016/j.neuroimage.2016.09.023 **This study demonstrates that the STN can be parcellated at 7 T into sub-regions with preferential white matter connectivity**.
42.• Tourdias T, Saranathan M, Levesque IR, Su J, Rutt BK. Visualization of intra-thalamic nuclei with optimized white-matter-nulled MPRAGE at 7T. Neuroimage. 2014;84:534–45. https://doi.org/10.1016/j.neuroimage.2013.08.069 **These authors report that 7 T can be used to visualize intra-thalamic nuclei, confirmed to be anatomically accurate**.
43. Verhagen R, Schuurman PR, van den Munckhof P, Contarino MF, de Bie RM, Bour LJ. Comparative study of microelectrode recording-based STN location and MRI-based STN location in low to ultra-high field (7.0 T) T2-weighted MRI images. J Neural Eng. 2016;13(6):066009. https://doi.org/10.1088/1741-2560/13/6/066009.
44.• Duchin Y, Abosch A, Yacoub E, Sapiro G, Harel N. Feasibility of using ultra-high field (7 T) MRI for clinical surgical targeting. PLoS One. 2012;7(5):e37328. https://doi.org/10.1371/journal.pone.0037328 **These authors report that image distortions at 7 T is comparable to 1.5 T for DBS targets.**
45. O'Gorman RL, Jarosz JM, Samuel M, Clough C, Selway RP, Ashkan K. CT/MR image fusion in the postoperative assessment of electrodes implanted for deep brain stimulation. Stereotact Funct Neurosurg. 2009;87(4):205–10. https://doi.org/10.1159/000225973.
46. Dula AN, Virostko J, Shellock FG. Assessment of MRI issues at 7 T for 28 implants and other objects. AJR Am J Roentgenol. 2014;202(2):401–5. https://doi.org/10.2214/AJR.13.10777.
47. Feng DX, McCauley JP, Morgan-Curtis FK, Salam RA, Pennell DR, Loveless ME, et al. Evaluation of 39 medical implants at 7.0 T. Br J Radiol. 2015;88(1056):20150633. https://doi.org/10.1259/bjr.20150633.
48. Boutet A, Hancu I, Saha U, Crawley A, Xu DS, Ranjan M, et al. 3-Tesla MRI of deep brain stimulation patients: safety assessment of coils and pulse sequences. J Neurosurg. 2019;2019:1–9. https://doi.org/10.3171/2018.11.JNS181338.
49. Hancu I, Boutet A, Fiveland E, Ranjan M, Prusik J, Dimarzio M, et al. On the (non-)equivalency of monopolar and bipolar settings for deep brain stimulation fMRI studies of Parkinson's disease patients. J Magn Reson Imaging. 2018. https://doi.org/10.1002/jmri.26321.
50. Haast RAM, Ivanov D, Uludag K. The impact of B1+ correction on MP2RAGE cortical T1 and apparent cortical thickness at 7T. Hum Brain Mapp. 2018;39(6):2412–25. https://doi.org/10.1002/hbm.24011.
51. Keuken MC, Isaacs BR, Trampel R, van der Zwaag W, Forstmann BU. Visualizing the human subcortex using ultra-high field magnetic resonance imaging. Brain Topogr. 2018;31(4):513–45. https://doi.org/10.1007/s10548-018-0638-7.
52. Yarach U, Luengviriya C, Stucht D, Godenschweger F, Schulze P, Speck O. Correction of B 0-induced geometric distortion variations in prospective motion correction for 7T MRI. MAGMA. 2016;29(3):319–32. https://doi.org/10.1007/s10334-015-0515-2.
53. Dimov AV, Gupta A, Kopell BH, Wang Y. High-resolution QSM for functional and structural depiction of subthalamic nuclei in DBS presurgical mapping. J Neurosurg. 2018:1–8. https://doi.org/10.3171/2018.3.JNS172145.
54. Liu C, Li W, Tong KA, Yeom KW, Kuzminski S. Susceptibility-weighted imaging and quantitative susceptibility mapping in the brain. J Magn Reson Imaging. 2015;42(1):23–41. https://doi.org/10.1002/jmri.24768.
55. Nolte IS, Gerigk L, Al-Zghloul M, Groden C, Kerl HU. Visualization of the internal globus pallidus: sequence and orientation for deep brain stimulation using a standard installation protocol at 3.0 Tesla. Acta Neurochir. 2012;154(3):481–94. https://doi.org/10.1007/s00701-011-1242-8.

56. Cobzas D, Sun H, Walsh AJ, Lebel RM, Blevins G, Wilman AH. Subcortical gray matter segmentation and voxel-based analysis using transverse relaxation and quantitative susceptibility mapping with application to multiple sclerosis. J Magn Reson Imaging. 2015;42(6):1601–10. https://doi.org/10.1002/jmri.24951.
57. Visser E, Keuken MC, Forstmann BU, Jenkinson M. Automated segmentation of the substantia nigra, subthalamic nucleus and red nucleus in 7T data at young and old age. Neuroimage. 2016;139:324–36. https://doi.org/10.1016/j.neuroimage.2016.06.039.
58. Keuken MC, Bazin PL, Backhouse K, Beekhuizen S, Himmer L, Kandola A, et al. Effects of aging on T(1), T(2)*, and QSM MRI values in the subcortex. Brain Struct Funct. 2017;222(6):2487–505. https://doi.org/10.1007/s00429-016-1352-4.
59. Keuken MC, Bazin PL, Schafer A, Neumann J, Turner R, Forstmann BU. Ultra-high 7T MRI of structural age-related changes of the subthalamic nucleus. J Neurosci. 2013;33(11):4896–900. https://doi.org/10.1523/JNEUROSCI.3241-12.2013.
60. Langkammer C, Schweser F, Shmueli K, Kames C, Li X, Guo L, et al. Quantitative susceptibility mapping: report from the 2016 reconstruction challenge. Magn Reson Med. 2018;79(3):1661–73. https://doi.org/10.1002/mrm.26830.
61. Zrinzo L, Zrinzo LV, Tisch S, Limousin PD, Yousry TA, Afshar F, Hariz MI Stereotactic localization of the human pedunculopontine nucleus: atlas-based coordinates and validation of a magnetic resonance imaging protocol for direct localization. Brain. 2008;131(Pt 6):1588–1598. https://doi.org/10.1093/brain/awn075.
62. Akram H, Dayal V, Mahlknecht P, Georgiev D, Hyam J, Foltynie T, et al. Connectivity derived thalamic segmentation in deep brain stimulation for tremor. Neuroimage Clin. 2018;18:130–42. https://doi.org/10.1016/j.nicl.2018.01.008.
63. Coenen VA, Allert N, Madler B. A role of diffusion tensor imaging fiber tracking in deep brain stimulation surgery: DBS of the dentato-rubro-thalamic tract (drt) for the treatment of therapy-refractory tremor. Acta Neurochir 2011;153(8):1579–1585; discussion 85. 10.1007/s00701-011-1036-z.
64. Kincses ZT, Szabo N, Valalik I, Kopniczky Z, Dezsi L, Klivenyi P, et al. Target identification for stereotactic thalamotomy using diffusion tractography. PLoS One. 2012;7(1):e29969. 10.1371/journal.pone.0029969.
65. Pouratian N, Zheng Z, Bari AA, Behnke E, Elias WJ, Desalles AA. Multi-institutional evaluation of deep brain stimulation targeting using probabilistic connectivity-based thalamic segmentation. J Neurosurg. 2011;115(5):995–1004. https://doi.org/10.3171/2011.7.JNS11250.
66. See AAQ, King NKK. Improving surgical outcome using diffusion tensor imaging techniques in deep brain stimulation. Front Surg. 2017;4:54. https://doi.org/10.3389/fsurg.2017.00054.
67. Vanegas-Arroyave N, Lauro PM, Huang L, Hallett M, Horovitz SG, Zaghloul KA, et al. Tractography patterns of subthalamic nucleus deep brain stimulation. Brain. 2016;139(Pt 4):1200–10. https://doi.org/10.1093/brain/aww020.
68.•• Horn A, Reich M, Vorwerk J, Li N, Wenzel G, Fang Q et al. Connectivity Predicts deep brain stimulation outcome in Parkinson disease. Ann Neurol. 2017;82(1):67–78. https://doi.org/10.1002/ana.24974. **This study shows that normative data can be used to predict clinical improvement in Parkinson's disease patients based on connectivity associated with the volume of tissue activated.**
69. Coenen VA, Allert N, Paus S, Kronenburger M, Urbach H, Madler B. Modulation of the cerebello-thalamo-cortical network in thalamic deep brain stimulation for tremor: a diffusion tensor imaging study. Neurosurgery. 2014;75(6):657–69. https://doi.org/10.1227/NEU.0000000000000540.
70. Coenen VA, Varkuti B, Parpaley Y, Skodda S, Prokop T, Urbach H, et al. Postoperative neuroimaging analysis of DRT deep brain stimulation revision surgery for complicated essential tremor. Acta Neurochir. 2017;159(5):779–87. https://doi.org/10.1007/s00701-017-3134-z.
71. Schlaepfer TE, Bewernick BH, Kayser S, Madler B, Coenen VA. Rapid effects of deep brain stimulation for treatment-resistant major depression. Biol Psychiatry. 2013;73(12):1204–12. https://doi.org/10.1016/j.biopsych.2013.01.034.
72. Sammartino F, Krishna V, King NK, Lozano AM, Schwartz ML, Huang Y, et al. Tractography-based ventral intermediate nucleus targeting: novel methodology and intraoperative validation. Mov Disord. 2016;31(8):1217–25. https://doi.org/10.1002/mds.26633.
73. Johansen-Berg H, Behrens TE, Sillery E, Ciccarelli O, Thompson AJ, Smith SM, et al. Functional-anatomical validation and individual variation of diffusion tractography-based segmentation of the human thalamus. Cereb Cortex. 2005;15(1):31–9. https://doi.org/10.1093/cercor/bhh105.
74. Krishna V, Sammartino F, Agrawal P, Changizi BK, Bourekas E, Knopp MV, et al. Prospective tractography-based targeting for improved safety of focused ultrasound thalamotomy. Neurosurgery. 2019;84(1):160–8. https://doi.org/10.1093/neuros/nyy020.
75. Riva-Posse P, Choi KS, Holtzheimer PE, Crowell AL, Garlow SJ, Rajendra JK, et al. A connectomic approach for subcallosal cingulate deep brain stimulation surgery: prospective targeting in treatment-resistant depression. Mol Psychiatry. 2018;23(4):843–9. https://doi.org/10.1038/mp.2017.59.
76. Tyagi H, Apergis-Schoute AM, Akram H, Foltynie T, Limousin P, Drummond LM, et al. A randomized trial directly comparing ventral capsule and anteromedial subthalamic nucleus stimulation in obsessive-compulsive disorder: clinical and imaging evidence for dissociable effects. Biol Psychiatry. 2019;85:726–34. https://doi.org/10.1016/j.biopsych.2019.01.017.
77. Anthofer J, Steib K, Fellner C, Lange M, Brawanski A, Schlaier J. The variability of atlas-based targets in relation to surrounding major fibre tracts in thalamic deep brain stimulation. Acta Neurochir. 2014;156(8):1497–504. https://doi.org/10.1007/s00701-014-2103-z.
78. Nowacki A, Schlaier J, Debove I, Pollo C. Validation of diffusion tensor imaging tractography to visualize the dentatorubrothalamic tract for surgical planning. J Neurosurg. 2018:1–10. https://doi.org/10.3171/2017.9.JNS171321.
79. Miocinovic S, Somayajula S, Chitnis S, Vitek JL. History, applications, and mechanisms of deep brain stimulation. JAMA Neurol. 2013;70(2):163–71. https://doi.org/10.1001/2013.jamaneurol.
80. Ewert S, Horn A, Finkel F, Li N, Kuhn AA, Herrington TM. Optimization and comparative evaluation of nonlinear deformation algorithms for atlas-based segmentation of DBS target nuclei. Neuroimage. 2019;184:586–98. https://doi.org/10.1016/j.neuroimage.2018.09.061.
81.•• Horn A, Li N, Dembek TA, Kappel A, Boulay C, Ewert S, et al. Lead-DBS v2: Towards a comprehensive pipeline for deep brain stimulation imaging. Neuroimage. 2019;(184):293–316. https://doi.org/10.1016/j.neuroimage.2018.08.068 **The authors report a streamline easy-to-use MATLAB-based platform to perform deep brain stimulation analysis.**
82. Chaturvedi A, Lujan JL, McIntyre CC. Artificial neural network based characterization of the volume of tissue activated during deep brain stimulation. J Neural Eng. 2013;10(5):056023. https://doi.org/10.1088/1741-2560/10/5/056023.
83. Schmidt C, Grant P, Lowery M, van Rienen U. Influence of uncertainties in the material properties of brain tissue on the probabilistic volume of tissue activated. IEEE Trans Biomed Eng.

2013;60(5):1378–87. https://doi.org/10.1109/TBME.2012.2235835.

84. Boutet A, Ranjan M, Zhong J, Germann J, Xu D, Schwartz ML, et al. Focused ultrasound thalamotomy location determines clinical benefits in patients with essential tremor. Brain. 2018;141(12):3405–14. https://doi.org/10.1093/brain/awy278.
85. Miguel EC, Lopes AC, McLaughlin NCR, Noren G, Gentil AF, Hamani C, et al. Evolution of gamma knife capsulotomy for intractable obsessive-compulsive disorder. Mol Psychiatry. 2019;24(2):218–40. https://doi.org/10.1038/s41380-018-0054-0.
86. Akram H, Sotiropoulos SN, Jbabdi S, Georgiev D, Mahlknecht P, Hyam J, et al. Subthalamic deep brain stimulation sweet spots and hyperdirect cortical connectivity in Parkinson's disease. Neuroimage. 2017;158:332–45. https://doi.org/10.1016/j.neuroimage.2017.07.012.
87.•• Dembek TA, Barbe MT, Astrom M, Hoevels M, Visser-Vandewalle V, Fink GR, et al. Probabilistic mapping of deep brain stimulation effects in essential tremor. Neuroimage Clin. 2017;13:164–73. https://doi.org/10.1016/j.nicl.2016.11.019 **This study demonstrates how to compute a probabilistic map of clinical outcomes using statistically validated techniques.**
88. Eisenstein SA, Koller JM, Black KD, Campbell MC, Lugar HM, Ushe M, et al. Functional anatomy of subthalamic nucleus stimulation in Parkinson disease. Ann Neurol. 2014;76(2):279–95 10.1002/ana.24204.
89. Butson CR, Cooper SE, Henderson JM, Wolgamuth B, McIntyre CC. Probabilistic analysis of activation volumes generated during deep brain stimulation. Neuroimage. 2011;54(3):2096–104. https://doi.org/10.1016/j.neuroimage.2010.10.059.
90. King NKK, Krishna V, Sammartino F, Bari A, Reddy GD, Hodaie M, et al. Anatomic targeting of the optimal location for thalamic deep brain stimulation in patients with essential tremor. World Neurosurg. 2017;107:168–74. https://doi.org/10.1016/j.wneu.2017.07.136.
91. Nowinski WL, Belov D, Pollak P, Benabid AL. Statistical analysis of 168 bilateral subthalamic nucleus implantations by means of the probabilistic functional atlas. Neurosurgery. 2005;57(4 Suppl):319–30 discussion -30.
92. Schupbach WMM, Chabardes S, Matthies C, Pollo C, Steigerwald F, Timmermann L, et al. Directional leads for deep brain stimulation: opportunities and challenges. Mov Disord. 2017;32(10):1371–5. https://doi.org/10.1002/mds.27096.
93. Hellerbach A, Dembek TA, Hoevels M, Holz JA, Gierich A, Luyken K, et al. DiODe: directional orientation detection of segmented deep brain stimulation leads: a sequential algorithm based on CT imaging. Stereotact Funct Neurosurg. 2018;96(5):335–41. https://doi.org/10.1159/000494738.
94. Hunsche S, Neudorfer C, Majdoub FE, Maarouf M, Sauner D. Determining the rotational orientation of directional deep brain stimulation leads employing flat-panel computed tomography. Oper Neurosurg (Hagerstown). 2019;16(4):465–70. https://doi.org/10.1093/ons/opy163.
95. Reinacher PC, Kruger MT, Coenen VA, Shah M, Roelz R, Jenkner C, et al. Determining the orientation of directional deep brain stimulation electrodes using 3D rotational fluoroscopy. AJNR Am J Neuroradiol. 2017;38(6):1111–6. https://doi.org/10.3174/ajnr.A5153.
96. Sitz A, Hoevels M, Hellerbach A, Gierich A, Luyken K, Dembek TA, et al. Determining the orientation angle of directional leads for deep brain stimulation using computed tomography and digital x-ray imaging: a phantom study. Med Phys. 2017;44(9):4463–73. https://doi.org/10.1002/mp.12424.
97. Anderson DN, Osting B, Vorwerk J, Dorval AD, Butson CR. Optimized programming algorithm for cylindrical and directional deep brain stimulation electrodes. J Neural Eng. 2018;15(2):026005. https://doi.org/10.1088/1741-2552/aaa14b.
98. Glasser MF, Sotiropoulos SN, Wilson JA, Coalson TS, Fischl B, Andersson JL, et al. The minimal preprocessing pipelines for the Human Connectome Project. Neuroimage. 2013;80:105–24. https://doi.org/10.1016/j.neuroimage.2013.04.127.
99. Yeo BT, Krienen FM, Sepulcre J, Sabuncu MR, Lashkari D, Hollinshead M, et al. The organization of the human cerebral cortex estimated by intrinsic functional connectivity. J Neurophysiol. 2011;106(3):1125–65. https://doi.org/10.1152/jn.00338.2011.
100. Horn A. The impact of modern-day neuroimaging on the field of deep brain stimulation. Curr Opin Neurol. 2019:1. https://doi.org/10.1097/WCO.0000000000000679.
101. Baldermann JC, Melzer C, Zapf A, Kohl S, Timmermann L, Tittgemeyer M, et al. Connectivity profile predictive of effective deep brain stimulation in obsessive-compulsive disorder. Biol Psychiatry. 2019;85:735–43. https://doi.org/10.1016/j.biopsych.2018.12.019.